RESEARCH ARTICLE

Flexible wearable biometric smart gloves based on friction nanogenerators

Xu Wang*

School of Arts and Science, Chengdu College, University of Electronic Science and Technology of China, Chengdu, Sichuan, China

Received: November 10, 2023; **accepted:** January 15, 2024.

Smart gloves are gloves with sensing devices that perceive the movements and touch of the hand through artificial intelligence technology and enable interaction with other devices. By wearing the device, it can autonomously recognize the user's movement intention and assist user in completing actions such as clenching fists and lifting objects. With the rapid development of internet technology, flexible wearable electronic devices have a wide range of applications in health supervision, motion detection, and other fields. To improve the power source performance of wearable electronic devices, this study proposed a flexible wearable biometric smart glove based on a friction nanogenerator. The study innovatively prepared a flexible wearable biometric smart device based on two different structures including traditional fabric and porous fiber and achieved multifunctional applications such as harvesting and signal sensing of external energy through friction nanogenerators. The results showed that there was a maximum average power at an external load resistance of 1 when the power density was about 3.98 mW/m^2. The devices short-circuit current was continuously stabilized at about 40 nA when the pressure magnitude was 10 N in the cycling experiment. When the frequency was varied in the interval from 1 to 4 Hz, the open circuit voltage magnitude was stable at around 57.8 V. The current in a short circuit had the highest value of about 0.4 μA when the frequency was 4 Hz. The classification accuracy rate of the smart glove for biometric recognition was as high as 98.3%. The results indicated that the smart glove designed in the study had good, stabilized performance and could operate for a long time, while having a high classification accuracy rate for biometric identification. The results provided new and improved ideas for the development and application of friction nanogenerators, and contributed to the creation of bendable wearable electronics.

Keywords: friction nanogenerator; flexible wearable; biometric; smart glove; fabric; porous fiber.

***Corresponding author:** Xu Wang, School of Arts and Science, Chengdu College, University of Electronic Science and Technology of China, Chengdu 610000, Sichuan, China. Email: Wangxu60306@163.com.

Introduction

The rapid development of the world economy has led energy to become a more important material basis and factor of production. While energy brings enormous economic benefits to mankind, it also inevitably brings various potential hazards to the environment. Therefore, the search for new, clean, and renewable power sources is a must for the modern economy's and society's sustained development. Currently, most products have been powered by external power sources [1, 2]. However, with the widespread adoption of wearable devices, the traditional power supply model is beginning to suffer from inevitable drawbacks, such as the inability to meet the long life span required by the devices and the lack of sustainability [3, 4]. In addition,

with the rapid development of science and technology, new energy technologies and smart wearable devices have become hot spots in research. Among them, triboelectric nanogenerator (TENG) technology, as a means of efficiently converting mechanical energy into electrical energy, has shown great potential in the fields of energy collection and sensors. The rapid development of biometric technology has brought new possibilities for personalized medicine and health monitoring. Among them, TENG uses the surface charge generated when two different materials come into contact and the electric field that changes with time to drive the flow of electrons in the external circuit. This power generation technology is capable of harvesting energy from the surrounding environment and converting mechanical energy into energy to drive wearable electronic applications [5]. Since its introduction, TENG has been used in several energy fields and has also received a lot of attention from researchers. Zhang's team conducted a comprehensive analysis on the development of fiber-based nanogenerators to enrich the research on nanogenerators. Strategies and principles for increasing the output capacity of nanogenerators made of fiber were summarized, and the results found that fiber-based nanogenerators could effectively mitigate the environmental pollution problem [6]. Luo *et al*. prepared a novel self-healing TENG by integrating polycaprolactone (PCL) material with flexible silver nanowires. The process utilized two electrodes with different structural properties to improve the self-healing capabilities of its friction surface and conductive layer. The results showed that the healable PCL polymeric material was able to self-repair by heating and softening, effectively extending the service life of the TENG [7]. An *et al*. suggested a system based on the self-powered system of the TENG. To address problems such as low conversion efficiency, various aspects such as mechanical structure and electrode materials were explored, while the applications of TENG in sensing and wearable devices were summarized. It was found that the high effective charge density of TENG could significantly improve the performance of self-powered systems [8]. Chen *et al*. analyzed multiple gallium nitride based semiconductors for the unclear energy transfer and conversion mechanism. The external output current always flew from GaN to Si or Al, which indicated that the interfacial electric field created by the friction charge really dominated the carrier transport direction [9].

On the other hand, the range of applications for flexible wearable devices is expanding. Zhu *et al*. proposed a flexible soft glove with multimodal feedback to reduce the complexity of glove system operation. The study designed a single basic structure with the improvement, and the results showed that the constructed glove system could detect hand movements in real time and recognize objects quickly, which significantly enhanced human perception [10]. Additional study proposed a portable smart pen integrated with a frictional potential shift vector sensor to enable tracking of human-computer interaction and biometric handwriting trajectories. The device could authenticate different users through their unique handwriting patterns, ultimately enabling improved human-machine interface and cyber security [11]. Wang and Qi conducted a series of econometric analysis of the relevant literatures to explore the fundamentals and research hotspots in the field of wearable devices. It was found that the current research focused on wearable devices spread across various aspects such as information acquisition and sensor materials. The application of wearable devices was beneficial for further applications of telemedicine and precision medicine in the future [12]. Huang *et al*. proposed a novel sensor power supply device to extend the duration of wearable gadgets' power supplies. The device achieved reliable and stable monitoring of the human body by generating uninterrupted power supply. The data showed that the wearable device was able to monitor the human body more accurately and present health reports in the device application [13]. TENG has become a popular technology in energy research due to its excellent performance and safety. The biometric

functions and power supply improvements of flexible wearable electronic devices have become urgently needed technologies at this stage.

The human body is constantly in motion, which generates abundant mechanical energy that can be harvested using TENG. With the development of technology, an important research direction for electronic devices is the realization of wearable and biometric functions. Current research in this specific field mainly focuses on TENG energy efficiency improvement, material innovation, and practical design of wearable devices. Although some progress has been achieved, there are still problems such as low energy conversion efficiency, poor device stability, and biometric recognition accuracy, which are in need to be improved. This research innovatively combined TENG with flexible fabrics to build a smart glove system that could achieve self-powering using multidisciplinary methods to improve energy conversion efficiency, enhance the stability and comfort of the equipment, and improve the accuracy of biometric identification. The results of this study not only promoted the development of TENG technology and biometric technology, but also had important impacts on different scientific fields including intelligent health monitoring, personalized medicine, and human-computer interaction. Through this proposed efficient and stable smart glove, humans could better achieve energy self-sufficiency while providing users with more accurate and convenient health monitoring services.

Materials and Methods

Friction generator based on starting effect

Nanogenerators are devices driven by the displacement currents in Maxwell's set of equations and can transform mechanical energy into electrical energy effectively [14]. Maxwell's displacement current was expressed in equation (1).

$$J_D = \frac{\partial D}{\partial t} = \varepsilon \frac{\partial E}{\partial t} + \frac{\partial P_s}{\partial t} \quad (1)$$

where *P* was the polarization field density. ε was the material's dielectric constant. ε_0 was the vacuum dielectric constant. *D* was the displacement field. *E* was the electric field. For homogeneous dielectrics, $P = (\varepsilon - \varepsilon_0)E, D = \varepsilon E$. TENG utilizes Maxwell's displacement current as its propelling force, converting mechanical energy into electrical energy. Unlike the conduction of free electron currents and considering the presence of polarized charges in dielectrics such as frictional and piezoelectric materials, the displacement currents have a polarized charge density due to the presence of surface electrostatic charges, thus yielding the modified Maxwell displacement current in equation (2).

$$J_D = \frac{\partial D}{\partial t} = \varepsilon_0 \frac{\partial E}{\partial t} + \frac{\partial P_s}{\partial t} \quad (2)$$

where P_s was the polarized charge density. $\varepsilon_0 \frac{\partial E}{\partial t}$ was the induced current generated by a varying electric field. $\frac{\partial P_s}{\partial t}$ was the current produced by the polarization field on the dielectric material's surface because of incoming electrostatic charge. When two materials with different polarities rub against each other, the same number of charges of opposite polarity will appear on their surfaces, a phenomenon known as the "frictional charging effect". Taking the example of the contact separation mode existing between two media, the electric field between the two media was expressed with the electric field at the gap in equation (3).

$$\begin{cases} E_{z1} = \sigma_1(z,t)/\varepsilon_1, E_{z2} = \sigma_1(z,t)/\varepsilon_2 \\ E_z = (\sigma_1(z,t) - \sigma_c)/\varepsilon_0 \end{cases} \quad (3)$$

where E_{z1} and E_{z2} were the electric fields existing between dielectric 1 and 2. E_z was the electric field at the gap between the two dielectrics'

separation. Based on this, the difference in the two electrodes' respective voltages was shown in equation (4).

$$V = \sigma_1(z,t)\left[\frac{d_1}{\varepsilon_1} + \frac{d_2}{\varepsilon_2}\right] + z\left[\sigma_1(z,t) - \sigma_c\right] / \varepsilon_0 \quad (4)$$

where *V* was the relative voltage difference. ε_1, ε_2 represented the dielectric constants of the two dielectrics. d_1 and d_2 were the thickness of the two dielectrics. $\sigma_1(z,t)$ represented the electrostatic field established by the frictional charge driving the flow of electrons through the external load, resulting in the electrodes' buildup of free electrons, as a function of the distance between the two dielectrics *z(t)*. If the dielectric was transformed for the relative voltage difference in the case of a short circuit, the transfer current density between the interiors of the different materials was obtained as below.

$$J_D = \frac{\partial D_z}{\partial t} = \frac{\partial \sigma_1(z,t)}{\partial t} = \sigma_c \frac{d_z}{d_t} \frac{d_1\varepsilon_0/\varepsilon_1 + d_2\varepsilon_0/\varepsilon_2}{\left[d_1\varepsilon_0/\varepsilon_1 + d_2\varepsilon_0/\varepsilon_2 + z\right]^2} + \frac{d\sigma c}{dt} \frac{z}{d_1\varepsilon_0/\varepsilon_1 + d_2\varepsilon_0/\varepsilon_2} \quad (5)$$

Because of the transport equation in the external circuit caused by the frictional electric field and the presence of the external load resistance, the density of the supplementary output current was obtained by Ohm's law in equation (6).

$$RA\frac{d\sigma_1(z,t)}{dt} = z\sigma_c/\varepsilon_0 - \sigma_1(z,t)\left[d_1/\varepsilon_1 + d_2/\varepsilon_2 + d_3/\varepsilon_3\right] \quad (6)$$

where *A* was the electrode's surface area. *z* was determined by the time of the applied force dynamic process t function.

Biometric keyboard based on flexible wearable fabrics

A biometric keyboard is a type of keyboard that utilizes biometric features for identity verification. It can confirm the user's identity by identifying their biometric features such as fingerprints, iris, and voiceprints, thereby enhancing the security of the system. To breakthrough the sensor technology based on flexible fabrics and to achieve the detection of human dynamic electrocardiogram (ECG) signals, the research combined TENG with flexible wearable sensor devices, resulting in a biometric keyboard that was self-powered, comfortable to wear, and having the advantages of human-computer interaction [15, 16]. Conventional fabrics are mostly made up of cotton, silk, and polyester insulating materials by means of weaving. The surface structure is not flat, which makes the preparation of continuous patterned conductive pole fabrics particularly difficult. To ensure the quality of the woven fabrics, this study choose to prepare bottom electrode fabrics by means of screen printing. A carbon nanotube (CNT) dispersion with the same properties but at a lower concentration of 0.16 wt/% was chosen to prepare the CNT fabric through a series of experiments. The pre-treated polyester fabric was placed in polytetrafluoroethylene solution (PTFE) and left to stand for 3 minutes before being placed in a blast drying oven for pre-drying at 70°C for 5 minutes. The process was repeated twice, and the polyester fabric was then dried at 150°C for 2 hours to obtain the friction layer. The entire device was sandwiched in a "sandwich" structure. The resulting CNT fabric was connected in series with the light-emitting diodes (LEDs) to a constant 3 v external power supply and the LEDs were able to emit light properly. The three-dimensional structure of the CNT in relation to the resistance was shown in Figure 1. The device's three components made up its overall resistance, namely the resistance of the bottom silver electrode ($R_{electrode}$), the contact resistance resulting from the contact interface between the CNT fabric and the bottom silver electrode ($R_{contact}$), and the resistance of the CNT fabric itself (R_{film}). The relationship between the three components and the total resistance (R_{total}) was shown in equation (7).

$$R_{total} \approx R_{electrode} + R_{contact} + R_{film} \quad (7)$$

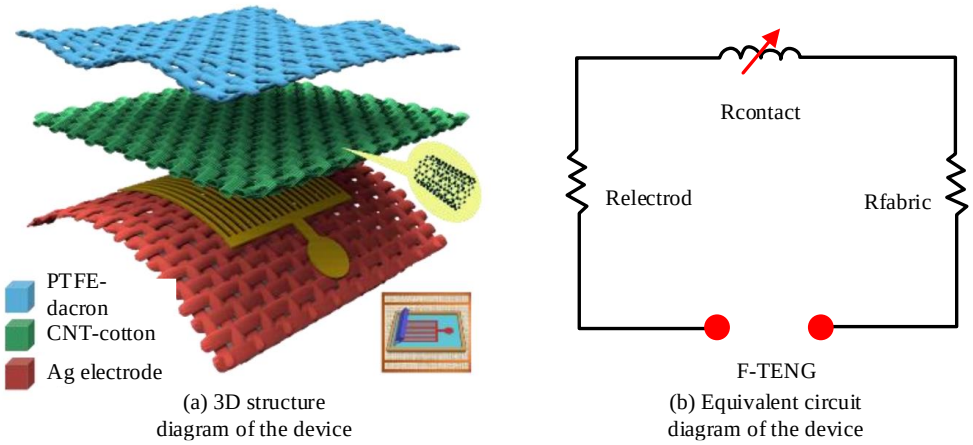

(a) 3D structure diagram of the device

(b) Equivalent circuit diagram of the device

Figure 1. The 3-D structure and equivalent circuit diagram of the device.

Due to the high electrical conductivity of the bottom silver electrode, the resistance present was much less than the remaining two resistances. A simplified resistance relationship was obtained in equation (8).

$$R_{total} \approx R_{contact} + R_{film} \tag{8}$$

Typically, the contact resistance has a higher value compared to CNT fabrics which, due to their greater flexibility and stretchability, are usually squeezed out of shape and thus become more compact. Using the capacitive model of TENG as a basis, a TENG circuit could be equated to a model of a capacitor, which denoted that a voltage V was placed between the capacitor's two electrode plates, at which point the capacitance changed over time causing the charge on the electrode plates Q to change, which in turn led to the external circuit's current flow, as expressed in equation (9).

$$I = \frac{dQ}{dt} = C\frac{dv}{dt} + V\frac{dc}{dt} = A\frac{d\sigma_1}{dt} \tag{9}$$

where *A* was the area of the metal electrode. σ_1 was the charge density induced by the metal electrode. When only the frequency of contact separation was varied, *A* was a constant. The charge density induced by the metal electrode per unit time, however, changed with frequency, so the final short-circuit current varied with frequency, further demonstrating the validity of the capacitance model [17]. Also, to further explore the applicability of the fabric TENG-flexible wearable biometric electronic device, the study used the fabric TENG as a self-driven pedometer device and stitched it together with a common commercial sock and wore it on the foot of a test subject. The study used the Fourier transform to analyze the resulting disparate raw electrical signals. The specific wavelet transform was shown in equation (10).

$$\begin{cases} W_{j,k}(f) = \int_{-\infty}^{+\infty} \psi_{j.k}(t) f(t) dt \\ f(t) = \psi_1(t) + \psi_2(t) + \psi_3(t) + \psi_4(t) \end{cases} \tag{10}$$

where $j(j = 1,2,3,4)$ was a positive integer. k was the number of variations at a given scale. $f(t)$ was the voltage signal in the corresponding original state. $\psi_1, \psi_2, \psi_3, \psi_4$ were the detailed components of the voltage decomposition.

Stretchable TENG-biometric smart glove based on a porous structure

Smart gloves are devices worn on the hands that can sense the movements and postures of the hands. It can recognize finger movements and gestures through built-in sensors and algorithms, thereby achieving interaction with computers or other intelligent devices. Combining a biometric

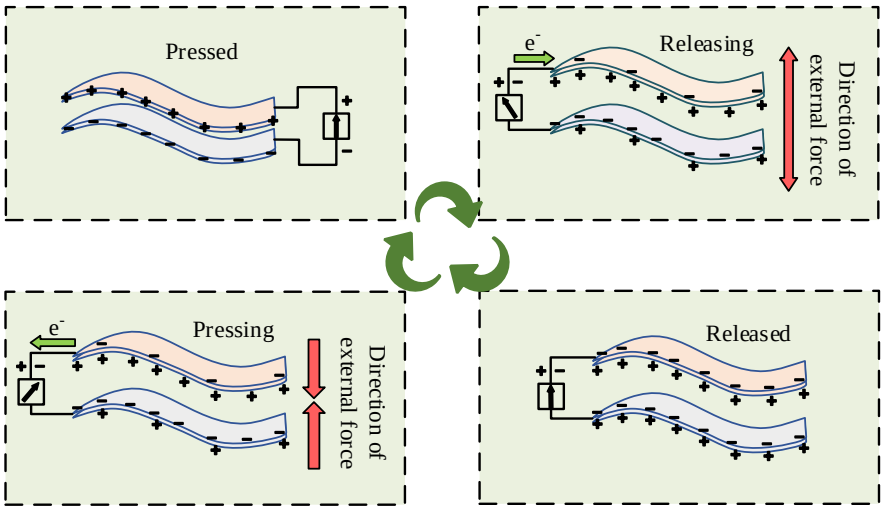

Figure 2. Principles of preparing the bottom electrode fabric by screen printing.

keyboard with smart gloves can achieve a more secure and convenient identity verification system. Users can authenticate their gestures by using smart gloves, and the system can verify their identity based on finger movements and postures. Meanwhile, biometric keyboards can be used for further verification, such as confirming the user's identity through fingerprints or voiceprints. This combined approach not only provides a higher level of security, but also provides a more natural and intuitive user experience. Flexible electronic devices require TENGs that can accommodate many forms of deformation, including bending, stretching, and shrinking. A stretchable fiber TENG with a porous structure had been designed and a stretchable electrode had been prepared by the template method, winding the yarn and a porous fiber with a diameter of only 2.5 mm [18] (Figure 2). During the actual movement of the human body, the amount of pressure exerted by the outside world was not fixed and therefore the TENG generated short-circuit current phenomena during its operation. A quantitative analysis of the changes in pressure and short-circuit current could be divided into two phases with different sensitivities. Equation (11) displayed the expression for the short-circuit current sensitivity.

$$S = \frac{\delta I}{\delta F} \times 100\% \tag{11}$$

where *S* was the short-circuit current sensitivity. δI was the amount of change in current. δF was the amount of change in external pressure. The definition of current was given in equation (12).

$$I = nesv \tag{12}$$

where *n* was the number of charges transferred in the circuit. *e* was the charge of the electrons. *s* was the cross-sectional area through the transferred charges. *v* was the speed at which the transferred charges move through the circuit (i.e. how fast the electrons are transferred). The *n*, *e*, *s* in the study were kept constant and the output power produced by the TENG on the corresponding load was only maximum when the external load and the TENG matched each other. The load power density was calculated using different sized resistors in series with this fiber and was shown in equation (13).

$$P = I^2 R / L \tag{13}$$

where *I* was the current flowing through the external load. *R* was the resistance associated

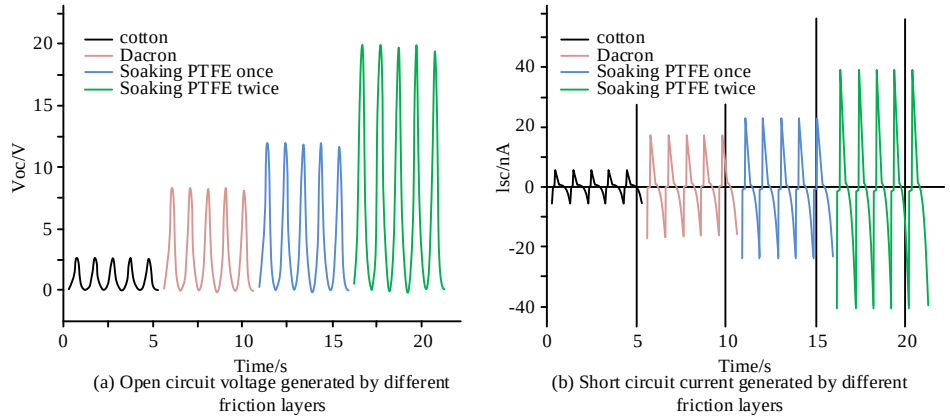

Figure 3. Contrasting the open circuit voltage and short circuit current in various scenarios.

with the external load. *L* was the length of the porous fiber. When the external load resistance was small, the external circuit must be short-circuited as the internal resistance of the TENG tended to positive infinity, so the change in current was always small and closer to zero even if the resistance to external stress was raised. The opposite was true when the external load had a high resistance. Based on TENG's capacitance model, it could be equated to the capacitance [19]. As the capacitance increased, the rate of increase of the voltage across the capacitor decreased. The energy stored in the capacitor at 100 s was calculated in equation (14).

$$E = \frac{1}{2}U^2 \times C \quad (14)$$

where *U* was the voltage across the capacitor. *C* was the size of the capacitor. It could be calculated that, when the time was 100 s and the size of the capacitor was 6.8 uF, the maximum energy stored by the capacitor could reach 0.51 mJ.

Results and discussion

Analysis of the electrical output performance of the TENG under different conditions

Since the constructed devices' electrical output performance is impacted by various friction layer materials, a total of four different friction layer materials were selected for comparison experiments. The four materials were untreated cotton fabric, untreated polyester fabric, polyester fabric soaked once in PTFE solution, and polyester fabric soaked twice in PTFE solution. Under the same circumstances, the fluctuation of open circuit voltage and short circuit current was investigated (Figure 3). The open circuit voltages produced by the various friction layers were shown in Figure 3a. The open-circuit voltages of the different friction layer materials were in a steady state at the corresponding times. The friction-generated open circuit voltage between the untreated cotton fabric and the skin on the human surface was 2.51 V during the 0-5 s. The open circuit voltage generated by friction between the untreated polyester fabric was 9.82 V during the 5-10 s. The open circuit voltage for the polyester fabric soaked once in PTFE solution was 11.95 V during the 10-15 s. The open circuit voltage for the 15-20 s showed the short-circuit currents generated by different friction layers (Figure 3b). As the material rubbed against human skin, the short-circuit current output showed a sharp change in the phenomenon. The minimum short-circuit currents for cotton, polyester, once-soaked and twice-soaked polyester fabrics were 5.12, -19.58, -22.34, and -40.97 nA, respectively. The results indicated that the electrical output of the twice-soaked polyester fabric was better, which might be due to the fact that PTFE was a highly electronegative substance in the sequence

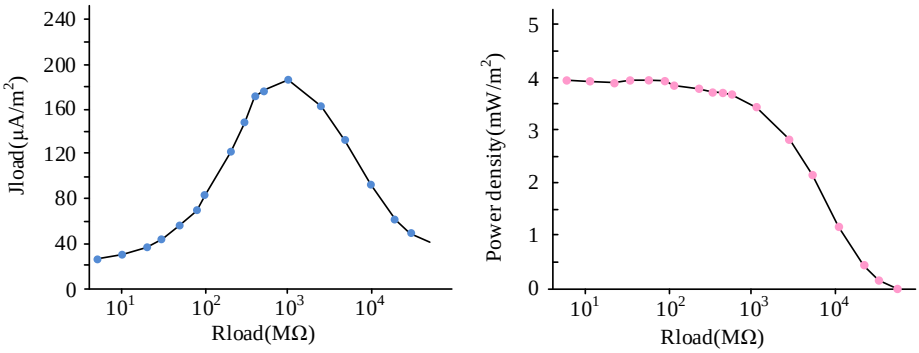

(a) The relationship between instantaneous current density and external load resistance

(b) The relationship between instantaneous power density and external load resistance

Figure 4. Output change curve of power at different resistances.

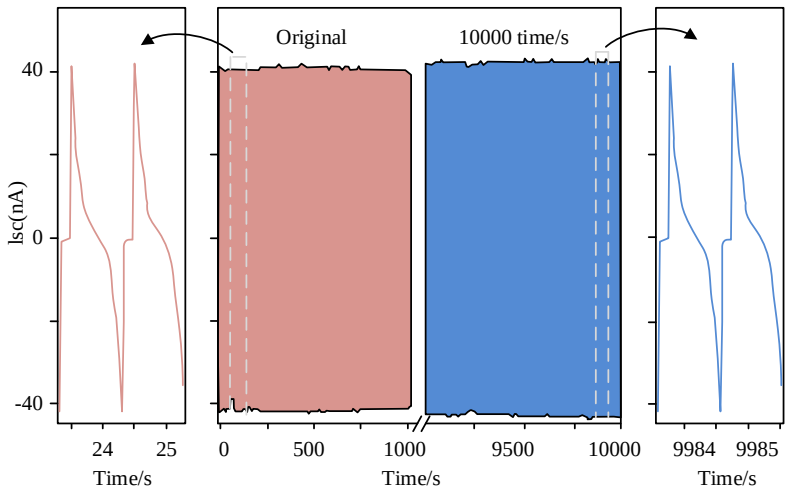

Figure 5. Cycling experiments of the device.

of frictional electricity and had better charge adsorption properties compared to the untreated polyester fabric versus the cotton fabric.

At the same time, under the change of pressure, the short-circuit current of the device exhibited a characteristic curve change (Figure 4). In the first stage, due to the porous structure of the fibers, TENG underwent significant deformation under small pressure changes, resulting in more frictional charges and short-circuit currents. When too much pressure was applied, the porous structure of the fibers was basically compressed, but due to the elasticity of the fiber silicone rubber material itself, the short-circuit current would still increase with the increase of pressure. In addition, the open-circuit voltage and short-circuit current produced by the device steadily increased with the increasing PTFE concentration. For the TENG, when the external load was compatible with the TENG, the maximum output power was accessible, so the power output of the different resistors was then analyzed. The instantaneous current density and power density in proportion to external load resistance was shown in Figure 5. As the resistance increased, the current first tended to a more stable state, and then began to drop rapidly. When the external load's resistance exceeds 100, the average output current was approximately 0. Meanwhile, the increase in

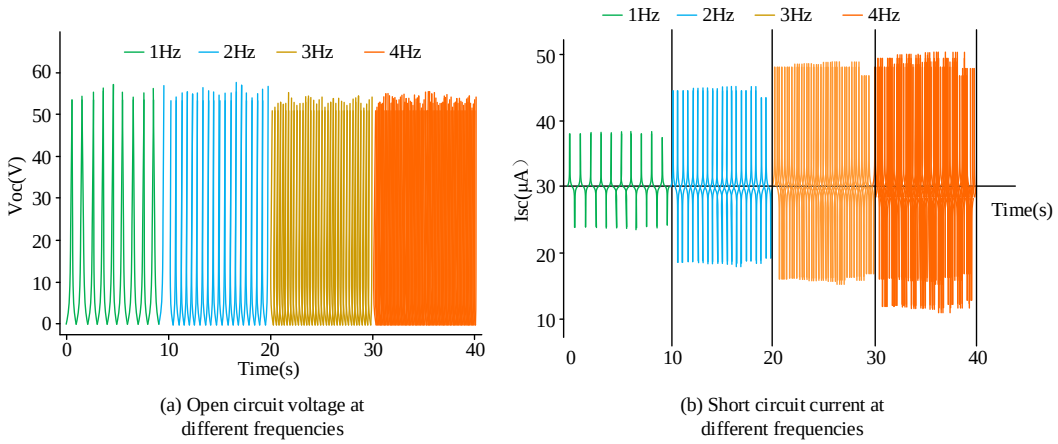

(a) Open circuit voltage at different frequencies

(b) Short circuit current at different frequencies

Figure 6. Short circuit current and open circuit voltage fluctuate at various frequencies.

resistance made the load power show a trend of rising and then falling. There was a maximum average power at a load resistance of 1 when the power density was about 3.98 mW/m^2. At the same time, the contact separation mode of the fabric TENG ensured that the electrical output generated by the device in each cycle came from contact electrification. Therefore, the cyclic experiment of the device was performed for testing. In the cyclic test, the conditions for each contact separation were not consistent with a pressure force of 10 N. As the number of contact separations increased, the magnitude of the short-circuit current did not change significantly and remained stable around 40 nA, which indicated that the designed equipment had good stability performance and could operate for a long time. In addition, the frequency of human movement was irregular and difficult to maintain consistency. The frequency loaded on the device was an important factor affecting the electrical output performance of the device. Therefore, the study gradually increased the frequency of loading pressure from 1 to 4 Hz to mimic the frequency of pressure generated by human movement. The open-circuit voltage hardly changed at all as the frequency continued to increase (Figure 6a). When the frequency was varied in the interval from 1 to 4 Hz, the open circuit voltage was around 57.8 V in size, which was probably because the amount of frictional charge generated in the friction layer was the same under the same pressure conditions and only when the frequency was changed, the amount of charge transferred between the two charges was also the same at this time, so the steady open circuit voltage between the two electrodes. The short-circuit current gradually started to increase as the frequency changes (Figure 6b). With a 4 Hz frequency, the short-circuit current had a maximum value of approximately 0.4 μA, probably because the open-circuit voltage increased when the resistance and other factors remained constant, causing the short-circuit current to increase.

Application of TENG-flexible wearable biometric smart gloves

TENG can use low frequency movements to convert mechanical energy generated by the human body into electrical energy to maintain the device in long term standby. The study analyzed the designed pressure-sensitive keypad of a smart glove by simulating human movement through a simple hand-tapping motion. A demonstration of a pressure-sensitive keyboard for a smart glove that consisted of four porous fibers as weft yarns (i = 1, 2, 3, 4) with three porous fibers as warp yarns (j = 5, 6, 7) were shown in Figure 7. Adjacent yarns were separated from each other using plain cotton threads to minimize interference with each other. The intersection of the warp and weft yarns was the key contact of the pressure

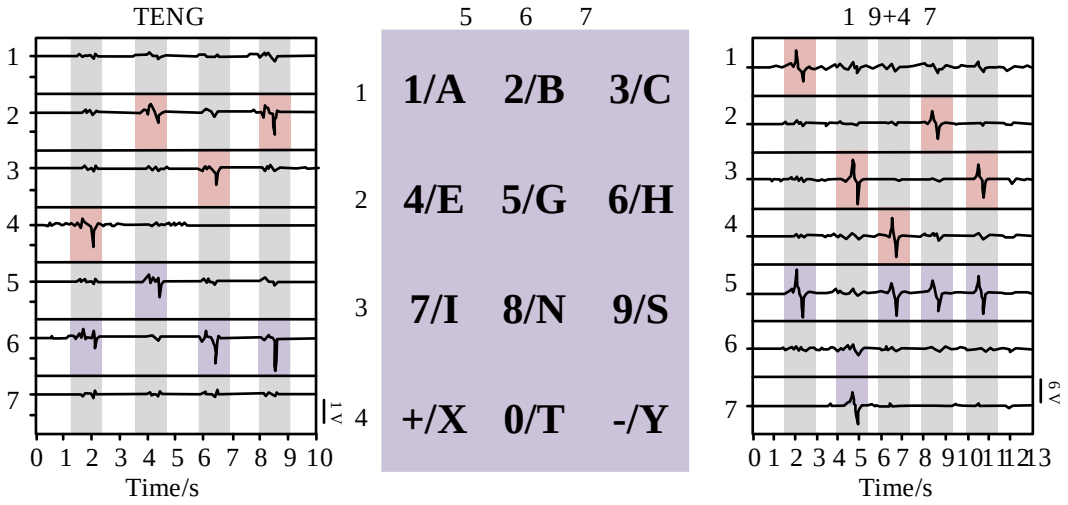

Figure 7. Out demonstration of pressure sensitive keyboard of smart gloves.

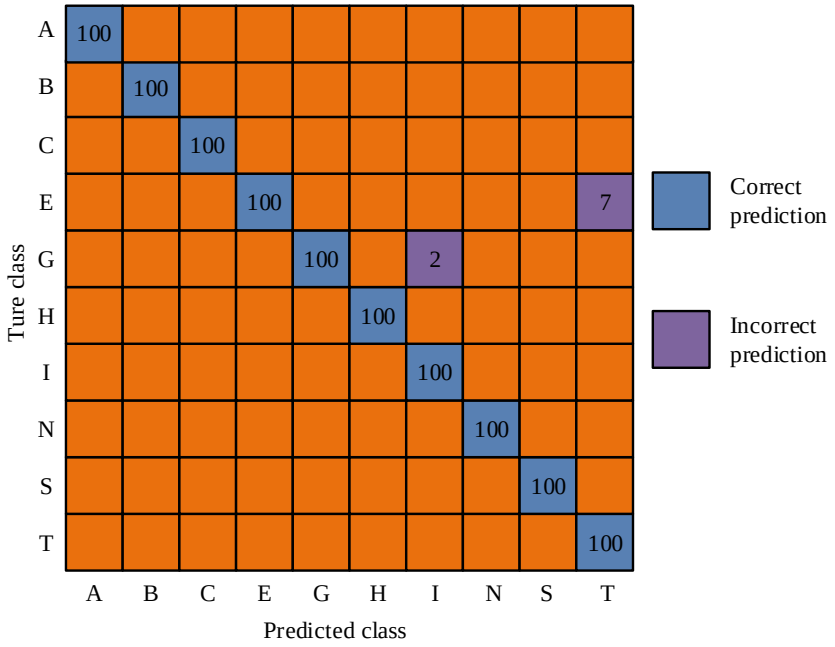

Figure 8. The confusion matrix of smart glove identification.

sensitive keypad inside each smart glove. When the letter "T" was pressed with the smart glove, the device generated the maximum voltage signal at the weft (i = 4) and warp (j = 6) respectively. Based on this particular property, it was determined that the position of the key was "0/T", which meant that the fabric keypad in the prepared smart glove had a high pressure sensitivity. When less finger pressure was applied, the output was displayed as a letter, while, when more pressure was applied, the smart keyboard was able to act as a wearable computing device. The research device was further applied to actual sign language operations for intelligent recognition of sign language. The confusion matrix of the smart

glove was demonstrated in Figure 8. The results showed that, when the actual gesture of the operator was E, there was a 7% probability that it would be incorrectly classified as gesture T, which was because the gestures of T and E were more similar, and the electrical signal output obtained from both would then be more similar. A comprehensive analysis of the classification effect of the research system showed that the prediction accuracy of the classification could reach 98.3%. To further verify the amount of pressure the smart glove could withstand in practice, the response of the voltage generated by the glove when placed under different external pressure conditions was studied. The results showed that, when the external pressure was 10 kPa, the maximum output voltage was 1.13 V. When the external pressure reached 22 kPa, the maximum output voltage was 3.92 V. When the external pressure reached 50 kPa, the maximum output voltage reached 4.11 V. From the overall change of the voltage curve, when the pressure was less than 22 kPa, the voltage output of the smart glove increased more. At pressures greater than 22 kPa, the TENG-Smart Glove voltage output signal increased less, which meant that the TENG had reached a limit in its ability to respond to higher pressures. 22 kPa of external pressure was sufficient to ensure that the TENG-Smart Glove was able to deliver the basic power required in everyday life. This further validated the stability of the smart glove's output, which had good prospects for application in the flexible electronics market.

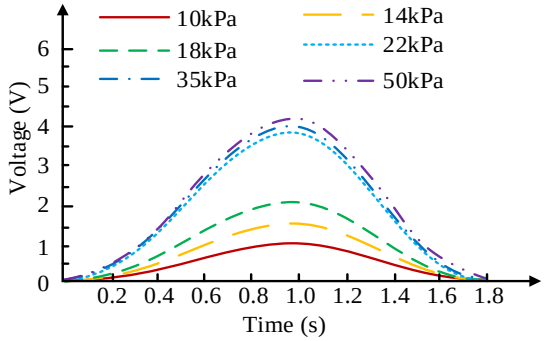

Figure 9. Voltage response of smart gloves under different external pressures.

Conclusion

To reduce the energy consumption of conventional electronic wearables, this study proposed a new self-powered system for flexible wearable biometric smart gloves based on TENG technology. The process was based on flexible fabric and porous fibers, respectively, to prepare a flexible wearable TENG and to collect electrical signal output for use in human-computer interaction among sensor applications, ultimately realizing the biometric function. The results showed that the twice soaked polyester fabric had better electrical output performance. When the frequency was 4 Hz, the short-circuit current was around 0.4 μA. The durability of the device and the resistance to water washing experiments did not show significant changes in the short-circuit current and open-circuit voltage generated by the device. When the resistance of the external load reached 100, the average output current was approximately 0. When the resistance of the external load was 1, there was the maximum average power with a power density of approximately 3.98 mW/m^2 (j = 6), which indicated that the key position was at "0/T". In terms of voltage response, the study device was able to respond to a pressure of 22 kPa and had good starting efficiency. All these results indicated that the electrical output of the research device was superior and could be used for versatile applications. However, the study was limited to the capture and energy harvesting of electrical signals from human movement and did not integrate the detection of various conditions such as temperature and humidity. Therefore, further research is needed to extend the experimental scope.

References

1. Singh S, Chauhan P, Singh NJ. 2020. Capacity optimization of grid connected solar/fuel cell energy system using hybrid ABC-PSO algorithm. Int J Hydrogen Energy. 45(16):10070-10088.
2. Kang SM, Lee HE, Wang HS, Shin JH, Jo W, Lee Y, *et al*. 2021. Self-powered flexible full-color display via dielectric-tuned hybrimer triboelectric nanogenerators. ACS Energy Lett. 6(11):4097-4107.

3. Barma M, Modibbo UM. 2022. Multiobjective mathematical optimization model for municipal solid waste management with economic analysis of reuse/ recycling recovered waste materials. JCCE. 1(3):122-137.
4. Cheng B, Xu Q, Ding Y, Bai S, Jia X, Yu Y, *et al*. 2021. High performance temperature difference triboelectric nanogenerator. Nat Commun. 12(1):1-8.
5. Shi Q, Dong B, He T, Sun Z, Zhu J, Zhang Z, *et al*. 2020. Progress in wearable electronics/photonics-Moving toward the era of artificial intelligence and internet of things. InfoMat. 2(6):1131-1162.
6. Zhang M, Du H, Liu K, Nie S, Xu T, Zhang X, *et al*. 2021. Fabrication and applications of cellulose-based nanogenerators. Adv. Compos. Hybrid Mater. 4(4):865-884.
7. Luo N, Feng Y, Wang D, Zheng Y, Ye Q, Zhou F, *et al*. 2020. New self-healing triboelectric nanogenerator based on simultaneous repair friction layer and conductive layer. ACS Appl Mater Interfaces. 12(27):30390-30398.
8. An X, Wang C, Shao R, Sun S. 2021. Advances and prospects of triboelectric nanogenerator for self-powered system. Int J Smart Nano Mater. 12(3):233-255.
9. Chen Y, Zhang Z, Wang Z, Bu T, Dong S, Wei W, *et al*. 2022. Friction-dominated carrier excitation and transport mechanism for GaN-based direct- current triboelectric nanogenerators. ACS Appl Mater Interfaces. 14(20):24020-24027.
10. Zhu M, Sun Z, Lee C. 2022. Soft modular glove with multimodal sensing and augmented haptic feedback enabled by materials' multifunctionalities. ACS Nano. 16(9):14097-14110.
11. He Q, Feng Z, Wang X, Wu Y, Yang J. 2022. A smart pen based on triboelectric effects for handwriting pattern tracking and biometric identification. ACS Appl Mater Interfaces. 14(43):49295-49302.
12. Wang C, Qi H. 2021. Visualising the knowledge structure and evolution of wearable device research. J Med Eng Technol. 45(3):207-222.
13. Huang J, Gu J, Liu J, Guo J, Liu H, Hou K, *et al*. 2021. Environmentally stable ionic organohydrogel as a self-powered integrated system for wearable electronics. J Mater Chem A. 9(30):16345-16358.
14. Wang Y, Adam ML, Zhao Y, Zheng W, Gao L, Yin Z, *et al*. 2023. Machine learning-enhanced flexible mechanical sensing. Nano-Micro Lett. 15(1):1-33.
15. Xiao X, Fang Y, Xiao X, Xu J, Chen J. 2021. Machine-learning-aided self-powered assistive physical therapy devices. ACS Nano. 15(12):18633- 18646.
16. Choudhuri S, Adeniye S, Sen A. 2023. Distribution alignment using complement entropy objective and adaptive consensus-based label refinement for partial domain adaptation. Artificial Intelligence and Applications. 1(1):43-51.
17. Shi Q, Yang Y, Sun Z, Lee C. 2022. Progress of advanced devices and internet of things systems as enabling technologies for smart homes and health care. ACS Mater Au. 2(4):394-435.
18. Zhang L, Cai H, Xu L, Ji L, Wang D, Zheng Y, *et al*. 2022. Macro-superlubric triboelectric nanogenerator based on tribovoltaic effect. Matter. 5(5):1532-1546.
19. Rui P, Zhang W, Wang P. 2021. Super-durable and highly efficient electrostatic induced nanogenerator circulation network initially charged by a triboelectric nanogenerator for harvesting environmental energy. ACS Nano. 15(4):6949-6960.